Varying the position of phospholipid acyl chain unsaturation modulates hopanoid and sterol ordering

Authors: Nguyen Ha Ngoc Anh[a], Liam Sharp[b], Edward Lyman[b] and James P Saenz[a]*

[a] Technische Universität Dresden, B CUBE Center for Molecular Bioengineering, 01307 Dresden, Germany

[b] Department of Physics and Astronomy, University of Delaware, DE 19716, Newark, Delaware

*corresponding author and lead contact: james.saenz@tu-dresden.de

ABSTRACT

The cell membrane acts as a responsive interface between the cell and its surroundings. Ultimately, the diverse panel of lipids comprising the lipidome are employed to tune membrane biophysical properties for optimal function. For eukaryotes, a family of amphiphiles called sterols are crucial due to their unique capacity to modulate the order of membrane lipids. Bacteria typically lack sterols, however, some can synthesize a family of sterol-analogues called hopanoids. Hopanoids are recognized as bacterial analogs of sterols due to their chemical and biophysical similarities. Notably, hopanoids are proposed as evolutionary sterol precursors since they have been found in ancient sediments and their biosynthesis could have proceeded prior to the oxygenation of Earth's surface. While hopanoids and sterols can both impart order to saturated phospholipids, this interaction changes vastly with the presence of a double bond in the phospholipid's acyl chain. Here, we present a study examining how the unsaturation position along the acyl chain influences the ordering effect of sterols (cholesterol) and hopanoids (diplopterol). We found that diplopterol and cholesterol exhibit different ordering effects on unsaturated lipids, depending on the relative positions of the double bond and the methyl groups of cholesterol/diplopterol. Moreover, in the bacterium *Mesoplasma florum*, diplopterol's interplay with unsaturated lipid isomers modulates bacterial membrane robustness. These results reveal how subtle changes in lipid structure can influence the membrane's collective properties and introduces double bond position as a modifiable lipidomic feature that cells can employ to fine-tune their membrane for adaptation to environmental change.

INTRODUCTION

Most living organisms share a common construct: the cell membrane. This thin bilayer of lipids defines the cell-environment interface, facilitating the cell's interactions with its surroundings. Not only does the bilayer layer protect against external physical and chemical perturbations, but it also serves as an organizational scaffold for cellular bioactivity. To support these functions, the membrane must modulate its biophysical properties to be simultaneously bioactive and mechanically robust. Ultimately, this is achieved through its lipid composition[1].

A biological membrane is made of a diverse mix of lipids, and each lipid's distinctive structure contributes to membrane's physical properties and functions. The main components of most membranes are phospholipids, a family of lipids with a hydrophilic head group and a hydrophobic, long

hydrocarbon chain called the acyl chain. Phospholipid acyl chain chemistry can influence membrane properties. For instance, acyl chains made of only single carbon-carbon bonds (or saturated lipids) create stiff membranes, while acyl chains with double bonds (or unsaturated lipids) make the membrane more fluid[2]. While each lipid's chemistry individually contributes to the membrane properties, their collective interactions also have an impact on the emergent properties of the membrane. A prime example of this is the role of sterols in Eukaryotes. These compounds have a planar ring system which acts as a scaffold supporting their packing with phospholipids[3,4]. When combined with saturated lipids, these lipid makes the membrane more diffusive, facilitating biological reactions. When combined with unsaturated lipids, sterols make the membrane more densely packed and robust against physical stresses[5,6]. In combination, cells employ lipid unsaturation as well as the ordering effect of sterols to modulate membrane properties.

Most non-eukaryotic organisms cannot synthesize sterols and must rely on other mechanisms to modulate their membrane properties[7,8]. Some bacteria utilize a family of compounds called hopanoids[9]. Hopanoids, like sterols, are tri-terpenoids and were discovered in the sedimentary record as early as 1.64 billion years ago[10]. Since both families are synthesized from squalene, with homologous enzymes (squalene-hopene cyclase and oxidosqualene cyclase)[11–13], they share certain chemical similarities. Like sterols, hopanoids also reside within the plasma membrane and contribute significantly to membrane robustness, permeability, and resistance against abiotic stresses[9,14–19]. For these reasons, hopanoids are considered both bacterial and ancient sterol analogs.

However, despite their similarities, hopanoids and sterols possess distinct properties. In the case of diplopterol (Dpop), a common hopanoid in bacteria, and cholesterol (Chol) a mammalian sterol both interact favorably with and condense saturated lipids, which is a diagnostic feature of lipid ordering[6]. However, the condensing effect of diplopterol is altered when an acyl chain unsaturation is introduced. For example, Chol condenses the unsaturated lipid 1,2-Dioleoyl-sn-glycero-3-phosphatidylcholine (Δ9-PC), while Dpop does not[6,20]. This observation highlighted a fundamental difference between Chol and Dpop interaction with unsaturated lipids. Interestingly, in 2020, Chwastek et al. investigated the lipidome of a hopanoid-bearing organism *Methylobacterium extorquens*, and found that the main unsaturation position was Δ11 instead of Δ9, with an additional Δ5 in cold-adapted lipidomes[21]. While the displacement of the double bond from Δ11 to Δ9 does not change the lipid individual's melting temperature significantly[22,23], the placement of the double bond has been shown to change Chol – lipid interaction in simulation and thus can affect the membrane's collective properties[24]. If this is the same case for Dpop, then perhaps bacteria's selection for double bond placement also modulates its membrane properties and could represent a mechanism of fine-tuning during temperature adaptation.

This study examines how the position of a double bond in the phospholipid acyl chain influences Dpop – lipid interactions. We show that while unsaturation position modulates both Dpop and Chol interaction with unsaturated lipids, they do so in distinct ways. Molecular dynamic simulations suggest that this difference stems from Dpop's methyl group distribution. Finally, we examine the effects of unsaturation position on Dpop/Chol–lipid interactions in the context of a biological membrane. In the bacteria *Mesoplasma florum*, the more favorable interaction between Δ11 and Dpop enhances the membrane's robustness against osmotic shock. Taken together, our work highlighted the link between lipid chemistry and lipid–lipid interactions, as well as its consequence for biomembrane robustness.

RESULTS

Chol and Dpop serve crucial roles in modulating membrane properties through their unique ability to influence the order of phospholipids within the bilayer. The interactions of Chol and Dpop with phospholipids can change significantly with acyl chain unsaturation, however, the effect of double bond position has rarely been discussed. We hypothesize that the position of double bonds along the phospholipid acyl chain impacts Chol/Dpop ordering, thus representing a constraint in the evolution of sterol- and hopanoid-containing lipidomes.

Phospholipid area exhibits small change with varying double bond position at physiological pressures

First, we investigated how double bond position influences the lipid packing density of three PC isomers with two mono-unsaturated chains with double bonds at Δ6, Δ9, Δ11 positions (Chemical structures are shown in Fig. 1A). While changing double bond position impacts lipid biophysical properties like melting temperature significantly[22,23], how the packing density (e.g. area) of these individual isomers varies has not been examined in vitro. Here, we employed a lipid monolayer model system to measure lipid packing density. In brief, lipids are assembled at an air–water interface where the surface area is slowly reduced to allow rearrangement to a compressible single layer of lipids (monolayer). The increase in ordering while compressing can be observed as an increase in surface pressure, allowing an estimation of the surface area of individual lipids in a monolayer.

The isotherms (surface pressure to area per lipid) of pure Δ6-, Δ9- and Δ11-PC are shown in Figure 1B. This isotherm reflects how lipid area changes from its liquid relaxed phase to a condensed phase, or from low surface pressure to high surface pressure. While values in the liquid relaxed phase might give information about miscibility, higher surface pressures (e.g. 30 mN/m) approach the pressures characteristic of biological membranes[25]. The differences in molecular area of the 3 isotherms were less than 3%. At 30 mN/m, the mean molecular area of Δ6-, Δ9-, and Δ11-PC were 65.3, 66.0, and 64.3 Å²/molecule, respectively. This suggested Δ9-PC was the largest, followed by Δ6-PC and Δ11-PC was the smallest, in accordance with a previously reported molecular dynamics simulation[26]. Our result demonstrated that varying double bond placement has a meager effect on the mean molecular area, despite having a huge impact on lipid melting temperature.

Both Chol and Dpop ordering are dependent on double bond position

We next examined how acyl chain double bond position impacts interaction of Chol and Dpop with phospholipids. We deposited mixtures of individual PC isomers and Chol or Dpop (the corresponding isotherms are shown in Figure 2A,B). At first glance, it is visible that isotherms of the mixtures diverge more across different double bonds compared with pure lipid isotherms. The trend shows that Δ11-PC has the lowest area per lipid, while Δ6- and Δ9-PC are more similar to one another.

One of the unique and diagnostic features of Chol is its ability to increase lipid packing density, which can be observed in a lipid monolayer through the so-called condensation effect[27]. In brief, a positive condensation effect occurs when a lipid mixture has a lower area than the area that would result from conservative mixing of the areas from the respective individual lipids. Consequently, the introduction of Chol to a phospholipid monolayer leads to a lower area of the lipid mixture than would be predicted from the observed areas of Chol and phospholipids. Condensation effects of Chol and Dpop were calculated according to the area per molecule values at 30 mN/m and reflected in Figure 2C. Here, Chol

consistently exhibited a condensing effect with unsaturated lipids regardless of the double bond position. In contrast, Dpop orders lipid isomers to a lesser extent, even negatively in the case of Δ9-DOPC. The data highlight the clear differences between the ordering effects of Chol and Dpop on unsaturated lipids with varying double bond positions.

While the condensation effect provides a functional readout of lipid packing efficiency, the monolayer also offers insights on how lipids interact thermodynamically through the calculation of the Gibbs free energy of interaction ΔG. ΔG reflects the affinity of 2 compounds for each other, in which the lower the ΔG, the more favorably two lipids interact[28]. ΔGs were calculated in 5 mN/m intervals and shown in Figure 2D. Chol interacted most favorably with Δ11-PC showing a ΔG of -1300 J/mol, comparable to the free energy of mixing of Chol with some saturated lipids[28]. Δ9- and Δ6-PC interaction with Chol were comparable and roughly 30% less favorable than with Δ11-PC. This data suggests that Chol has a preference for double bonds positioned further away from the head group, however from the limited data here the relationship does not appear to be linear. In contrast, the interaction between Dpop and PC isomers diverged from those observed with Chol. The Δ6-PC and Dpop mixture yielded ΔG of approximately 0 reflecting perfect mixing. Δ9-PC had a positive ΔG indicating a repulsive interaction. Interestingly, Δ11-PC yielded a ΔG of -100k/J revealing that only Δ11-PC interacted favorably with Dpop. This trend is completely different compared with the pattern observed with Chol, piquing interest in the investigation into the forces governing these interactions.

Together, these observations indicate that double bond position strongly influences the lipid ordering effect of both Chol and Dpop. While all isomers interact favorably with Chol with only some quantitative differences, that is not the case for Dpop. By moving the double bond just 2 carbons from Δ11 to Δ9, the interaction changes from favorable to unfavorable, potentially destabilizing the membrane. It is thus important to gain a deeper understanding of this phenomenon as well as its consequences on biological membranes.

Dpop methyl group distribution mediates interactions with unsaturated lipids

While Δ9 and Δ11 are two unsaturation sites most commonly found in nature[29–31], our in vitro experiments showed that they interacted completely differently with Dpop. To gain molecular insight into this variance, we performed *in silico* analyses using molecular dynamic simulations. We first considered the ordering effect of Dpop to individual acyl chains through the deuterium order parameter S_{CD}[32]. In brief, S_{CD} describes the relative orientation of the C-H bond relative to the bilayer normal. Higher S_{CD} values correspond to more ordered acyl chain conformations.

To ground-truth our model results, we first considered the interaction of Dpop with saturated DPPC since this is well-characterized. Dpop orders saturated lipids comparably to Chol[6]. Fig 3A investigated the interaction between Dpop and DPPC (1,2-dipalmitoyl-sn-glycero-3-phosphatidylcholine) at temperatures above and below the melting transition temperature of DPPC. As the concentration of Dpop increased, both acyl chains of DPPC displayed higher order, indicating the effect of Dpop consistent with our previous experimental observations[6,33]. This effect was more prominently seen in the liquid rather than gel phase. Next, we considered lipids with sn-1 saturated and sn-2 unsaturated acyl chains (Fig 3B). Interestingly, Dpop showed a larger ordering effect for the saturated chain relative to the unsaturated chain, suggesting that the interaction of Dpop with lipids containing asymmetrically unsaturated acyl chains may exhibit different collective properties than with lipids containing all saturated or unsaturated acyl chains. We then considered how Dpop's ordering effect varies with

double bond position in the unsaturated chain. In the sn-2 position, Δ11 was ordered more similarly to saturated chains than Δ9, suggesting a higher ordering of Dpop for the individual Δ11 chain. In PC with unsaturation in both acyl chains, we observed that chain position (sn-1 or sn-2) imparted little effect on ordering. Rather, the position of the double bond was critical in determining the acyl chain's order when interacting with Dpop (Fig 3C). Ordering was higher for Δ11-PC compared with Δ9-PC, similar to what we saw in the monolayer system.

In a previous simulation, Martinez-Seara et al. highlighted how PC's double bond and Chol's methyl group placement impacted the ordering effect[24]. We thus investigate the placement of PC's double bond relative to the positions of methyl groups extending from the Dpop ring structure. We focused on the methyl groups annotated in Fig 1A due to their rleative proximity to acyl chain unsaturations. Figure 4 describes the probability of placement of π bonds and methyl group in the z-axis, vertical from the membrane plane, with 0 being the center of the hydrophobic region. Between the 2 lipid mixes, there was a displacement of individual methyl groups of Dpop, most visibly in the M1 position, suggesting Dpop–lipid interactions rearranged molecules and methyl group placement. More importantly, Δ9-PC's double bond seemed to align with methyl group M2, while Δ11-PC double bond did not co-localize with other methyl groups. Given a repulsive Van der Waals forces between the π bond and the methyl group, this alignment might explain the reduced condensing effect observed for Δ9-PC, while Dpop and Δ11-PC interacted more favorably. This interplay between lipid structure and membrane biophysics provides insights that could be extended to other sterols and hopanoids, possibly laying a path for predicting how hopanoid/sterol and phospholipid structure collectively influence membrane properties.

Dpop different interaction to unsaturation sites affect *Mesoplasma florum* susceptibility to osmotic shock

So far, we have established that the interaction of Dpop with phospholipids changes across double bond isomers. To investigate how this variation in lipid–lipid interaction can affect biomembrane properties, we employed *Mesoplasma florum* as a living model system. *M. florum* is a Mollicute with no cell wall and a minimal genome[34–36]. With limited machinery, Mesoplasma cannot synthesize its own lipids and relies on supplemented lipids from the media, offering a straightforward way to manipulate its lipidomes. Previously characterized as Acholeplasma, this bacterium is not sterol-dependent[37]. By introducing either Δ9- or Δ11-PC to its lipid diet, we can create two identical biological membrane systems differing only in their unsaturation site. We then investigated this system to explore the effect of lipid–lipid interactions on a cellular scale.

Traditionally cultured with an undefined lipid diet in serums, we first test Mesoplasma's ability to grow in a defined lipid diet comprised of egg sphingomyelin, palmitic acid, and the addition of either Dpop or Chol, and Δ9- and/or Δ11-PC. Figure 5A displays the cellular lipid content, indicating that Dpop/Chol were incorporated into the cell. We measured Mesoplasma's growth through the proxy of media pH acidification with phenol red signal[38]. The growth rate recorded in Figure 5B suggested all diets sustained *Mesoplasma florum*'s growth. Mesoplasma grew faster when supplemented with Δ9-PC rather than Δ11-PC, in both combinations with Dpop or Chol.

Since Chol ordering of unsaturated lipids has previously been associated with membrane robustness, we tested Mesoplasma membrane robustness with osmotic shock. Live cells were harvested and resuspended in hypoosmotic conditions. As water from outside the cell rushes inwards to equilibrate

osmolarity, the cell expands and the membrane is stressed and ruptures. This rupture then exposes cellular DNA to propidium iodide, a dye that cannot penetrate intact membranes, but which fluoresces when it interacts with DNA. By quantifying the fluorescence intensity, we estimated the fraction of cells lysed due to osmotic shock, and consequently assayed membrane robustness. Figure 5C shows the cell's susceptibility to osmotic shock when supplied with different lipid diets. When cells were supplied with Chol, the addition of Δ9- or Δ11-PC did not produce significant changes in cellular robustness. However, cells fed with Δ9-PC and Dpop exhibited higher susceptibility that cells fed with Δ11-PC and Dpop. This data suggested that Dpop and Δ9-PC unfavorable interaction counteracts Dpop's ability to bolster membrane robustness.

DISCUSSION

Most organisms require unsaturated lipids for membrane fluidity. Several desaturation pathways have evolved to synthesize double bond positioned at Δ9 or Δ11[29–31]. While these two double bond positions might be selected due to their significant effect in lowering lipid melting temperature (from the fully saturated phospholipid)[22,23], the biological distinctions between the two positions remain elusive. Why would life have evolved two different pathways for lipids with nearly identical properties? Our study first investigated the area and packing density of individual unsaturated lipid isomers. While Δ9-PC displayed a larger area per lipid than other PC isomers, the change was small, consistent with previous simulations[26]. Similarly lipid packing density showed negligible changes, suggesting that a key difference might lie in the interaction with other lipids.

Cholesterol and diplopterol are both prevalent lipids, accounting for more than 40% of their respective membrane lipidomes[21,39]. Our data suggested both these components interact with unsaturated lipids in a double bond position-dependent manner. While cholesterol condenses all unsaturated isomers, diplopterol can only condense Δ11-PC, albeit less potently than cholesterol. Further simulations suggest this difference stems from the interaction of the isoprenoid's methyl group and the phospholipid's double bond. For diplopterol, its interaction with unsaturated lipids is significantly hindered by having multiple methyl groups extending from both sides of the cyclic ring, similar to biosynthetic precursor to cholesterol, lanosterol[40–43]. Notably, when the double bond resides in Δ9 position, and its distribution overlaps with the methyl group M2, it prevents effective diplopterol packing, resulting in a stark contrast between diplopterol's repulsive interaction with Δ9-PC and favorable interaction with Δ11-PC.

From these observations, we hypothesize that the differentiation between Δ9 and Δ11 might be the most significant in hopanoid-bearing organisms. We probed this lipid–lipid interaction in the bacteria *Mesoplasma florum* and found that the favorable interaction of Δ11-PC and diplopterol enhanced membrane resilience to osmotic shock compared to Δ9-PC. This is an indicator of a more robust membrane against physical stress, as well as a potential mechanism for osmoadaptation, which hopanoids were previously shown to play a critical role in soil and plant associated bacteria[44,45]. Indeed, multiple hopanoid-bearing bacteria have Δ11 as the monounsaturation site[29], instead of Δ9 in eukaryotes. Our observations, however, show that this preference is not crucial for cholesterol-bearing organisms. Cholesterol exhibits efficient packing with all isomers tested, leading to comparable membrane robustness against osmotic shock. This might difference might have alleviated any evolutionary selection against Δ9 in early sterol-bearing organisms, providing more flexibility to produce lipids with double bond positions optimized for orthogonal lipid-lipid or lipid-protein

interactions. Our results, therefore, suggest that a transition from hopanoid to sterol-containing lipidomes could have widened the chemical landscape available for cells to explore in assembling their membranes.

The acyl chain's double bond position can provide benefits in other cellular contexts as well. we previously observed that when challenged with extreme cold temperatures (e.g. below 15 C) *Methylobacterium extorquens* introduces a double bond in the Δ5 position[21]. Considering that the Δ5 unsaturation would have a negligible effect on the fluidity of the membrane, it was not clear why *M. extorquens* would employ this modification during cold adaptation. Our current observations indicate that a Δ5 unsaturation could disrupt diplopterol ordering thereby compensating for reduced fluidity at lower temperatures. This phenomenon introduces a potential mechanism for membrane fine-tuning membrane fluidity via diplopterol–lipid interactions.

In summary, our research elucidates how the placement of phospholipid unsaturation modulates the condensing effect of cholesterol or diplopterol, and potentially other sterols and hopanoids. These lipid-lipid interactions influence membrane properties such as robustness, potentially introducing selection pressures on the position of double bonds dictated by the reliance on either sterols or hopanoids as ordering lipids. Moreover, shifting double bonds along the acyl chain can fine-tune membrane properties for adaptation to environmental conditions such as cold temperature or osmotic stress. Our findings emphasize the complexity of lipid-lipid interactions and underscore how subtle structural variations in lipids can influence collective membrane properties.

METHODS

MATERIALS

Δ6-, Δ9-, Δ11-PC and egg sphingomyelin were purchased from Avanti Polar Lipids. Chol and palmitic acid were purchased from Sigma, and Dpop from Chiron. Stock concentrations of lipids were measured by phosphate assay. Chol and Dpop were weighed out on a precision scale and solubilized in a known volume of chloroform.

MONOLAYER

Chloroform solutions of pure lipids and mixtures were prepared at 0.2 mg/mL lipid concentrations. Monolayers were prepared by injecting 15-30 µL of lipid solution onto an aqueous subphase maintained at 25°C by a built-in temperature-controlled circulating water bath. The subphase was comprised of 10 mM Hepes, 150 mM NaCl, pH to 7. Isotherms were recorded using a 70 cm^2 teflon Langmuir trough fitted with a motorized compression barrier equipped with pressure sensor (Kibron DeltaPi).

The mean molecular area (MMAs) for each mixture were estimated from the averages of isotherms from three monolayers that were prepared independently. Data were rounded down to the nearest neighbor for condensation effect and free energy calculation. All isotherms were fitted to a regression, and statistical significance was tested using manova with the 2 coefficients.

The condensation effect was calculated as follows:

$$c = 100 - \frac{A_0}{X1A1 + X2A2} (\%)$$

Where c = % condensation, A_o = the MMA of the lipid mixture, X_1, X_2 = the mole fraction of lipid 1 and 2 in the mix, and A_1, A_2 = the MMAs of lipid 1 and 2 at surface pressures 30 mN/m. Error bars were produced based on error propangation.

The ΔG was calculated by integrating the areas of lipid mixtures over pressures Π = 5, 10, 15, 20, and 25 mN/m according to Grzybek et al[25]. Error bars were produced based on error propagation.

DIPLOPTEROL MODEL DEVELOPMENT

A CHARMM compatible model for diplopterol (Dpop) was developed using the automated atom typing and parameter assignment pipeline CGenFF.[30] Charmm topology and parameter files are provided as Supplemental Material.

SIMULATION COMPOSITION AND CONSTRUCTION

Simulation systems contained either DOPC or POPC (unsaturation at either the Δ6, Δ9, or Δ11 position) and one of either Dpop or Chol. All initial configurations were built using the CHARMM-GUI webserver.[47–49] Systems containing atypical unsaturated chains (Δ6 or Δ11) were generated by first building a binary mixture of the corresponding Δ9 lipid (DOPC or POPC) with either Dpop or Chol, then "mutating" the unsaturated chain(s) to move the double bond to the appropriate position, using a Charmm script provided by the Klauda Lab (Univ. of Maryland; script provided in Supplemental Materials).

All simulations contained approximately 550 lipids per leaflet and at least 50 TIP3P[50] water molecules per lipid. All lipids were modeled with the CHARMM36 force-field,[51] except Dpop which was modeled using CGenFF as described above. Initial dimensions in the membrane plane were about 17.5 nm x 17.5 nm, containing approximately 270,000 atoms. Initial structures of 1,2-Dioleoyl-sn-glycero-3-phosphocholine (DOPC) and 1-Palmitoyl-2-oleoyl-sn-glycero-3-phosphocholine (POPC) were constructed using CHARMM-GUI. Simulations box sizes used 50 water molecules per lipid using TIP3 water.

Eight different binary mixtures were simulated: Δ6-DOPC: Dpop, Δ9-DOPC: Dpop, Δ11 DOPC: Dpop, Δ9-POPC: Dpop, Δ11 POPC: Dpop, Δ6-DOPC:Chol, Δ11-DOPC:Chol, and Δ11-POPC:Chol. Each binary mixture was simulated at four different compositions: 95:5, 85:15, 70:30, 50:50. Each binary system was simulated for 500 nsec of production simulation as described below. 5 additional controls were simulated without any sterol or hopanoid, each for 50 nsec of production simulation as described below: Δ6-DOPC, Δ9-DOPC, Δ11-DOPC, Δ9-POPC, Δ11-POPC.

EQUILIBRATION AND PRODUCTION SIMULATIONS

Each system was prepared individually for production simulation through a series of 6 minimization and heating steps as provided by the CHARMM-GUI equilibration protocol: (i) steepest descent to minimize the initial configuration; (ii) 125,000 steps of leapfrog dynamics with a 1 fsec timestep and velocities reassigned every 500 steps; (iii) 125,000 steps of leapfrog dynamics with a 1 fsec timestep, pressure controlled by the Parinello-Rahman barostat[52] and velocities reassigned every 500 steps, then a total of 750,000 steps of leapfrog dynamics with a 2 fsec timestep and hydrogen positions constrained by LINCS,[53] pressure controlled by the Parinello-Rahman barostat,[52] and velocities reassigned every 500 steps. During equilibration, double bonds were restrained in the *cis* configuration to prevent isomerization; these restraints are gradually reduced during the final three stages of the equilibration protocol. Production simulations (NPT ensemble) were integrated with leapfrog using the Parinello-Rahman[52] barostat to control pressure (time constant 5 psec; compressibility 4.5e−5 bar−1; coupled anisotropically to allow independent fluctuation of the in-plane and normal directions) and temperature controlled using Nose-Hoover[54,55] (time constant 1 psec) at a temperature of 298 °C.

Hydrogens were constrained with LINCS (expansion order 4), a 2 fsec timestep was used, short range electrostatics were computed directly within 1.2 nm, and long-range electrostatics were computed every timestep using particle mesh Ewald[56,57] with a grid spacing of 1 Å and cubic interpolation. Long range dispersion was smoothly truncated over 10-12 nm using a force-switch cutoff scheme. Simulations that included DPOP used Gromacs 2020.4, while simulations that included were run on a different resource and used Gromacs 2018.3.

CALCULATION OF SIMULATION OBSERVABLES

The angle between either Dpop or Chol and the membrane normal, defining the orientation of both by a vector from atom C24 to atom O3 (see Supplemental Figure SXX). The locations of methyl groups in Dpop or Chol along the direction normal to the membrane were recorded and compiled into histograms with a bin size of 0.87 Å. Deuterium order parameters were obtained from the simulations via $S_{CD} = \frac{1}{2}\langle 3cos^2(\phi) - 1\rangle$, where ϕ is the angle between the C-H bond vectors along the hydrocarbon chain. They were computed with the orderparam2.tcl script produced by Justin Gullingsrud. The area per lipid was calculated using the Voronoi construction implemented in MEMBPLUGIN.[58] The location of each lipid is defined by the center of geometry of the C2, C21, and C31 atoms and the location of the Chol/ Dpop was defined by the O3 atom, and then a Voronoi construction is built around these points in the plane parallel to the membrane surface.

CELL CULTURE

Mesoplasma florum L1 strains were grown in a modified, lipid-free SP4 media with components as follows (per 1L): Bacto Tryptone 10g, Bacto Peptone 5.3g, PPLO 3.5g, BSA 5.95g, Yeastoleate 2g, D-Glucose 5g, sodium bicarbonate 3.15g, L-Glutamine 0.05g, Penicillin G-sodium salt 0.645g, phenol red 11 mg/L, pH to 7.0 and filtered. Lipid diet was added separately prior to passaging at concentration: Dpop, Chol 5 mg/L, egg sphingomyelin 25 mg/L, palmitic acid 10 mg/L, Δ9- and Δ11-PC 12.5 mg/L for the corresponding diets. Cells were grown in glass flasks and incubated at either 30°C with shaking at 60 rpm. Growth was recorded using phenol red media pH detection through absorbance at 562nm using a 10mm cuvette (DeNovix DS-11 FX+). Growth rate was defined as negative of the slope of the linearly fitted trendline in the indicative range of phenol red (OD562nm from 0.75 – 0.4).

MEMBRANE INCORPORATION

Cells were collected in early exponential stage and centrifuged (5000 rcf, 7 min, 30°C). Supernatant were discarded and cell pellet was washed with wash buffer (200 mM NaCl, 25 mM HEPES, 1% glucose, pH 7.0) and centrifuged (5000 rcf, 7 min, 30°C). The collected pellet was then subjected to a Bligh Dyer extraction[59]. Briefly, the pellet was homogenized in a mixture of water:chloroform:methanol in 0.8:1:2 ratio and sonicated for 2 minutes. Subsequently, water and chloroform were added in 1:1 ratio. The mixture was sonicated for 2 minutes, and centrifuged at 2000 rcf for 30 seconds in a mini centrifuge to promote phase separation. The lower, organic fraction containing lipids was collected and transferred to a fresh tube. The total lipid extract was then deposited on a silica gel plate (Supelco) and placed in a glass chamber. Chromatography was first performed using chloroform as the running phase, then chloroform:methanol:water (65:35:4) as the running phase to half plate length. After the run, the plate was dried and stained using 8 % copper sulphate in 3% phosphoric acid solution and heated until visible bands were observed. Images were captured using a GelDoc (Biozym Azure c600) and analysed using ImageJ.

MEMBRANE OSMOTIC SHOCK

Cells were collected in early exponential stage and centrifuged (5000 rcf, 7 min, 30°C). The collected pellet was resuspended in a serial dilution of 0%, 20%, 40%, 60%, 80% and 100% of wash buffer (200 mM NaCl, 25 mM HEPES, 1% glucose, pH 7.0). The suspension was stained with 10 uM propidium iodide and added to a 96-well plate. Fluoresence emission was recorded using a Tecan Spark fluorescence reader, with excitation at 529 – 549 nm and emission at 609 – 629 nm. The fraction of cell lysed was calculated by normalizing the signal of each sample to the 0% and 100% wash buffer sample.

REFERENCES

1. Harayama, T. & Riezman, H. Understanding the diversity of membrane lipid composition. *Nature Reviews Molecular Cell Biology* vol. 19 281–296 (2018).
2. Harayama, T. & Antonny, B. Beyond Fluidity: The Role of Lipid Unsaturation in Membrane Function. *Cold Spring Harb. Perspect. Biol.* a041409 (2023) doi:10.1101/cshperspect.a041409.
3. Yeagle, P. L. Cholesterol and the cell membrane. *Biochim. Biophys. Acta BBA - Rev. Biomembr.* **822**, 267–287 (1985).
4. Bloch, K. E. Sterol, Structure and Membrane Function. *Crit. Rev. Biochem.* **14**, 47–92 (1983).
5. Adaptive Lipid Packing and Bioactivity in Membrane Domains | PLOS ONE. https://journals.plos.org/plosone/article?id=10.1371/journal.pone.0123930.
6. Sáenz, J. P., Sezgin, E., Schwille, P. & Simons, K. Functional convergence of hopanoids and sterols in membrane ordering. *Proc. Natl. Acad. Sci. U. S. A.* **109**, 14236–14240 (2012).
7. Wei, J. H., Yin, X. & Welander, P. V. Sterol synthesis in diverse bacteria. *Front. Microbiol.* **7**, (2016).
8. Fischer, W. W., Summons, R. E., Pearson, & A. *Targeted genomic detection of biosynthetic pathways: anaerobic production of hopanoid biomarkers by a common sedimentary microbe*. *Geobiology* vol. 3 33–40 www.tigr.org/tigr-scripts/CMR2/GenomePage3.spl?database= (2005).
9. Belin, B. J. *et al.* Hopanoid lipids: From membranes to plant-bacteria interactions. *Nature Reviews Microbiology* vol. 16 304–315 (2018).
10. Brocks, J. J. *et al.* Biomarker evidence for green and purple sulphur bacteria in a stratified Palaeoproterozoic sea. *Nature* **437**, 866–870 (2005).
11. Lenhart, A. *et al.* Binding Structures and Potencies of Oxidosqualene Cyclase Inhibitors with the Homologous Squalene−Hopene Cyclase. *J. Med. Chem.* **46**, 2083–2092 (2003).
12. Ermondi, G. & Caron, G. GRIND-based 3D-QSAR to predict inhibitory activity for similar enzymes, OSC and SHC. *Eur. J. Med. Chem.* **43**, 1462–1468 (2008).
13. Racolta, S., Juhl, P. B., Sirim, D. & Pleiss, J. The triterpene cyclase protein family: A systematic analysis. *Proteins Struct. Funct. Bioinforma.* **80**, 2009–2019 (2012).
14. Kulkarni, G. *et al.* Specific Hopanoid Classes Differentially Affect Free-Living and Symbiotic States of Bradyrhizobium diazoefficiens. *mBio* **6**, 10.1128/mbio.01251-15 (2015).
15. Ricci, J. N., Morton, R., Kulkarni, G., Summers, M. L. & Newman, D. K. Hopanoids play a role in stress tolerance and nutrient storage in the cyanobacterium Nostoc punctiforme. *Geobiology* **15**, 173–183 (2017).
16. Brenac, L., Baidoo, E. E. K., Keasling, J. D. & Budin, I. Distinct functional roles for hopanoid composition in the chemical tolerance of Zymomonas mobilis. *Mol. Microbiol.* **112**, 1564–1575 (2019).
17. Bradley, A. S. *et al.* Hopanoid-free Methylobacterium extorquens DM4 overproduces carotenoids and has widespread growth impairment. *PLOS ONE* **12**, e0173323 (2017).
18. Rizk, S. *et al.* Functional diversity of isoprenoid lipids in Methylobacterium extorquens PA1. *Mol. Microbiol.* **116**, 1064–1078 (2021).
19. Kannenberg, E. L. & Poralla, K. Hopanoid Biosynthesis and Function in Bacteria. *Naturwissenschaften* **86**, 168–176 (1999).
20. Methylation at the C-2 position of hopanoids increases rigidity in native bacterial membranes | eLife. https://elifesciences.org/articles/05663.
21. Chwastek, G. *et al.* Principles of Membrane Adaptation Revealed through Environmentally Induced Bacterial Lipidome Remodeling. *Cell Rep.* **32**, (2020).

22. Knothe, G. & Dunn, R. O. A Comprehensive Evaluation of the Melting Points of Fatty Acids and Esters Determined by Differential Scanning Calorimetry. *JAOCS J. Am. Oil Chem. Soc.* **86**, 843–856 (2009).
23. Quinn, P. J. The fluidity of cell membranes and its regulation. *Prog. Biophys. Mol. Biol.* **38**, 1–104 (1981).
24. Martinez-Seara, H. *et al.* Interplay of unsaturated phospholipids and cholesterol in membranes: Effect of the double-bond position. *Biophys. J.* **95**, 3295–3305 (2008).
25. Grzybek, M., Kubiak, J., \Lach, A., Przyby\lo, M. & Sikorski, A. F. A raft-associated species of phosphatidylethanolamine interacts with cholesterol comparably to sphingomyelin. A Langmuir-Blodgett monolayer study. *PLoS ONE* **4**, (2009).
26. Martinez-Seara, H. *et al.* Effect of double bond position on lipid bilayer properties: Insight through atomistic simulations. *J. Phys. Chem. B* **111**, 11162–11168 (2007).
27. Demel, R. A., Van Deenen, L. L. M. & Pethica, B. A. Monolayer interactions of phospholipids and cholesterol. *Biochim. Biophys. Acta BBA - Biomembr.* **135**, 11–19 (1967).
28. Almeida, P. F. F. Thermodynamics of lipid interactions in complex bilayers. *Biochim. Biophys. Acta - Biomembr.* **1788**, 72–85 (2009).
29. Fulco, A. J. Fatty acid metabolism in bacteria. *Prog. Lipid Res.* **22**, 133–160 (1983).
30. From zero to six double bonds: phospholipid unsaturation and organelle function - PubMed. https://pubmed.ncbi.nlm.nih.gov/25906908/.
31. Bloch, K. Enzymic synthesis of monounsaturated fatty acids. *Acc. Chem. Res.* **2**, 193–202 (1969).
32. Schindler, H. & Seelig, J. Deuterium order parameters in relation to thermodynamic properties of a phospholipid bilayer. Statistical mechanical interpretation. *Biochemistry* **14**, 2283–2287 (1975).
33. Sáenz, J. P. *et al.* Hopanoids as functional analogues of cholesterol in bacterial membranes. *Proc. Natl. Acad. Sci. U. S. A.* **112**, 11971–11976 (2015).
34. Baby, V. *et al.* Inferring the Minimal Genome of Mesoplasma florum by. *mSystems* **3**, 1–14 (2018).
35. Lachance, J. *et al.* Genome-scale metabolic modeling reveals key features of a minimal gene set. *Mol. Syst. Biol.* **17**, 1–20 (2021).
36. Matteau, D. *et al.* Integrative characterization of the near-minimal bacterium Mesoplasma florum. *Mol. Syst. Biol.* **16**, 1–25 (2020).
37. McCoy, R. E., Basham, H. G. & Tully, J. G. Acholeplasma florum, a new species isolated from plants. *Int. J. Syst. Bacteriol.* **34**, (1984).
38. Matteau, D. *et al.* Integrative characterization of the near-minimal bacterium Mesoplasma florum. *Mol. Syst. Biol.* **16**, 1–25 (2020).
39. Lorent, J. H. *et al.* Plasma membranes are asymmetric in lipid unsaturation, packing and protein shape. *Nat. Chem. Biol.* **16**, 644–652 (2020).
40. Urbina, J. A. *et al.* Molecular order and dynamics of phosphatidylcholine bilayer membranes in the presence of cholesterol, ergosterol and lanosterol: a comparative study using 2H-, 13C- and 31P-NMR spectroscopy. *Biochim. Biophys. Acta BBA - Biomembr.* **1238**, 163–176 (1995).
41. Smondyrev, A. M. & Berkowitz, M. L. Molecular Dynamics Simulation of the Structure of Dimyristoylphosphatidylcholine Bilayers with Cholesterol, Ergosterol, and Lanosterol. *Biophys. J.* **80**, 1649–1658 (2001).
42. Sabatini, K., Mattila, J.-P. & Kinnunen, P. K. J. Interfacial Behavior of Cholesterol, Ergosterol, and Lanosterol in Mixtures with DPPC and DMPC. *Biophys. J.* **95**, 2340–2355 (2008).
43. Bui, T. T., Suga, K. & Umakoshi, H. Roles of Sterol Derivatives in Regulating the Properties of Phospholipid Bilayer Systems. *Langmuir* **32**, 6176–6184 (2016).

44. Tookmanian, E. M., Belin, B. J., Sáenz, J. P. & Newman, D. K. The role of hopanoids in fortifying rhizobia against a changing climate. *Environ. Microbiol.* **23**, 2906–2918 (2021).
45. Tookmanian, E. *et al.* Hopanoids Confer Robustness to Physicochemical Variability in the Niche of the Plant Symbiont Bradyrhizobium diazoefficiens. *J. Bacteriol.* **204**, e00442-21 (2022).
46. Vanommeslaeghe, K. *et al.* CHARMM general force field: A force field for drug-like molecules compatible with the CHARMM all-atom additive biological force fields. *J. Comput. Chem.* **31**, 671–690 (2010).
47. Jo, S., Kim, T., Iyer, V. G. & Im, W. CHARMM-GUI: A web-based graphical user interface for CHARMM. *J. Comput. Chem.* **29**, 1859–1865 (2008).
48. CHARMM-GUI Input Generator for NAMD, GROMACS, AMBER, OpenMM, and CHARMM/OpenMM Simulations Using the CHARMM36 Additive Force Field | Journal of Chemical Theory and Computation. https://pubs.acs.org/doi/10.1021/acs.jctc.5b00935.
49. Wu, E. L. *et al.* CHARMM-GUI Membrane Builder toward realistic biological membrane simulations. *J. Comput. Chem.* **35**, 1997–2004 (2014).
50. Price, D. J. & Brooks, C. L. A modified TIP3P water potential for simulation with Ewald summation. *J. Chem. Phys.* **121**, 10096–10103 (2004).
51. Update of the CHARMM All-Atom Additive Force Field for Lipids: Validation on Six Lipid Types | The Journal of Physical Chemistry B. https://pubs.acs.org/doi/10.1021/jp101759q.
52. Parrinello, M. & Rahman, A. Polymorphic transitions in single crystals: A new molecular dynamics method. *J. Appl. Phys.* **52**, 7182–7190 (1981).
53. LINCS: A linear constraint solver for molecular simulations - Hess - 1997 - Journal of Computational Chemistry - Wiley Online Library. https://onlinelibrary.wiley.com/doi/10.1002/(SICI)1096-987X(199709)18:12%3C1463::AID-JCC4%3E3.0.CO;2-H.
54. Nosé, S. A molecular dynamics method for simulations in the canonical ensemble. *Mol. Phys.* **52**, 255–268 (1984).
55. Hoover, W. G. Canonical dynamics: Equilibrium phase-space distributions. *Phys. Rev. A* **31**, 1695–1697 (1985).
56. Darden, T., York, D. & Pedersen, L. Particle mesh Ewald: An N·log(N) method for Ewald sums in large systems. *J. Chem. Phys.* **98**, 10089–10092 (1993).
57. A smooth particle mesh Ewald method | The Journal of Chemical Physics | AIP Publishing. https://pubs.aip.org/aip/jcp/article/103/19/8577/180219/A-smooth-particle-mesh-Ewald-method.
58. Guixà-González, R. *et al.* MEMBPLUGIN: studying membrane complexity in VMD. *Bioinformatics* **30**, 1478–1480 (2014).
59. Bligh, E. G. & Dyer, W. J. A RAPID METHOD OF TOTAL LIPID EXTRACTION AND PURIFICATION.

Figures

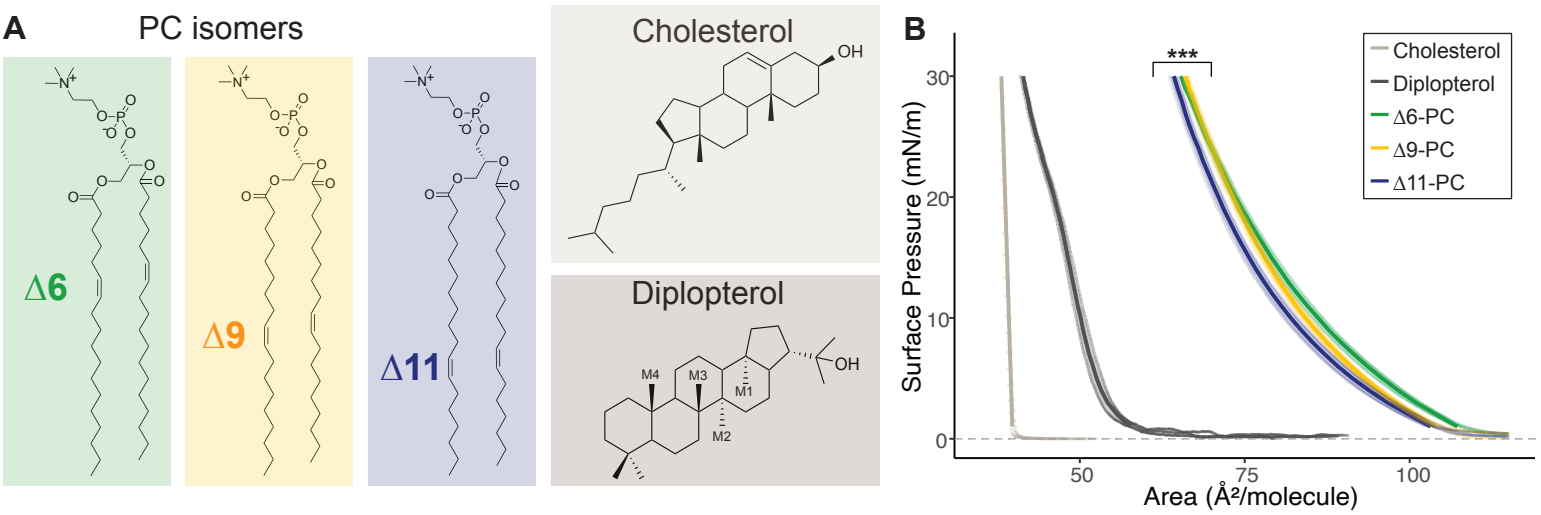

Fig 1. (A) Chemical structure of di-unsaturated PC isomers, Chol and Dpop and (B) Isotherms of the corresponding lipids at 20 °C, *** (F=12.4, p < 0.0005).

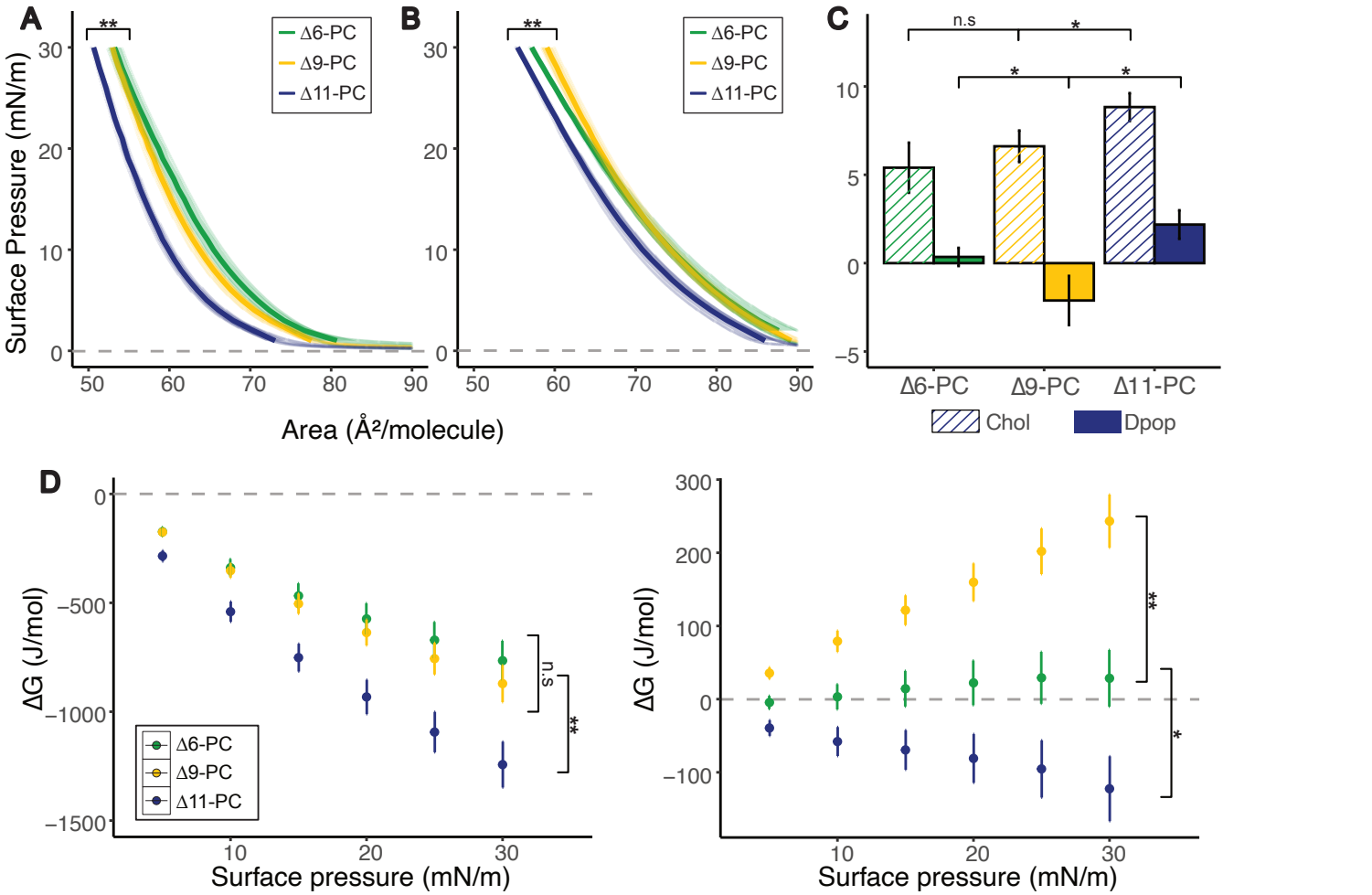

Fig 2. PC isomers interact differently with Chol and Dpop. While Chol ordering of PC increases as double bond position is shifted further from the headgroup, Dpop only exhibits an ordering effect with Δ11-PC. (A) Isotherms of PC isomers mixed with Chol (2:1) at 20°C. ** (F=7.75, p < 0.005) manova (B) Isotherms of PC mixture with Dpop (2:1) at 20°C. ** (F=8.18, p < 0.005) manova (C) Condensing effect of Chol and Dpop calculated the ordering effect on PC isomers at high surface pressure (30 mN/m). Error bar represents standard deviation. n.s (p > 0.5) * (p < 0.05) unpaired t-test (D) Energy of interaction (ΔG) of lipid pairs during compression. Error bar represents standard deviation. n.s (p > 0.5) * (p < 0.05) ** (p < 0.005) unpaired t-test.

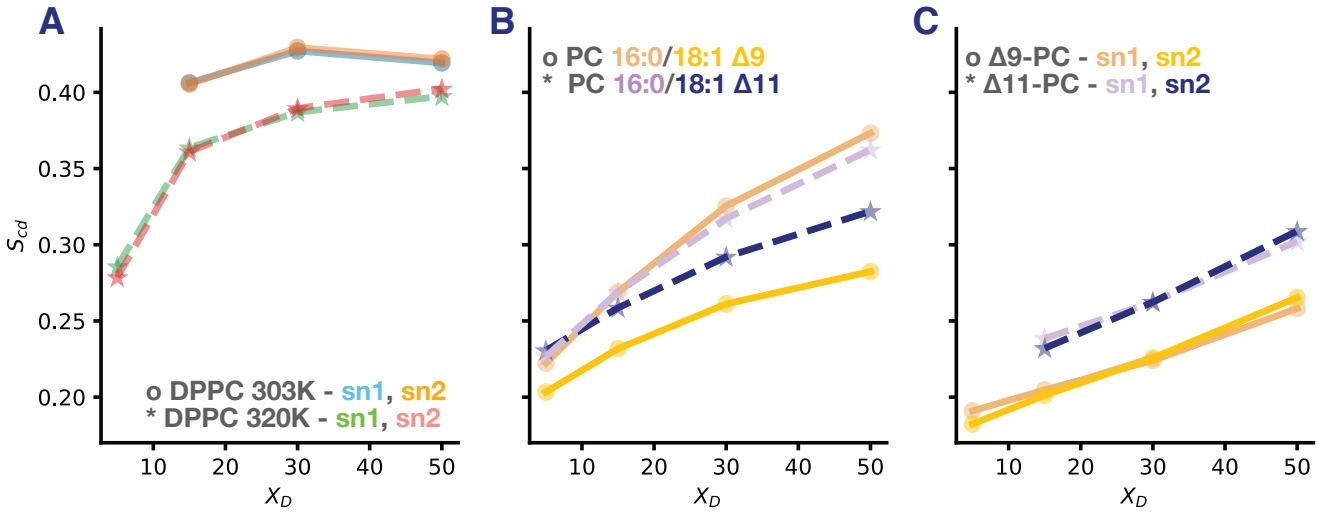

Fig 3. Molecular dynamic simulations show Dpop orders 18:1 Δ11 more efficiently than 18:1 Δ9. (A) Dpop ordering effect with saturated DPPC were confirmed by S_{CD}. (B) Dpop ordered saturated chains most efficiently, then 18:1 Δ11 and the least for 18:1 Δ9. (C) Dpop's ordering effect was similar regardless of sn chain position, but depended on double bond position, with Δ11 a greater ordering effect than Δ9.

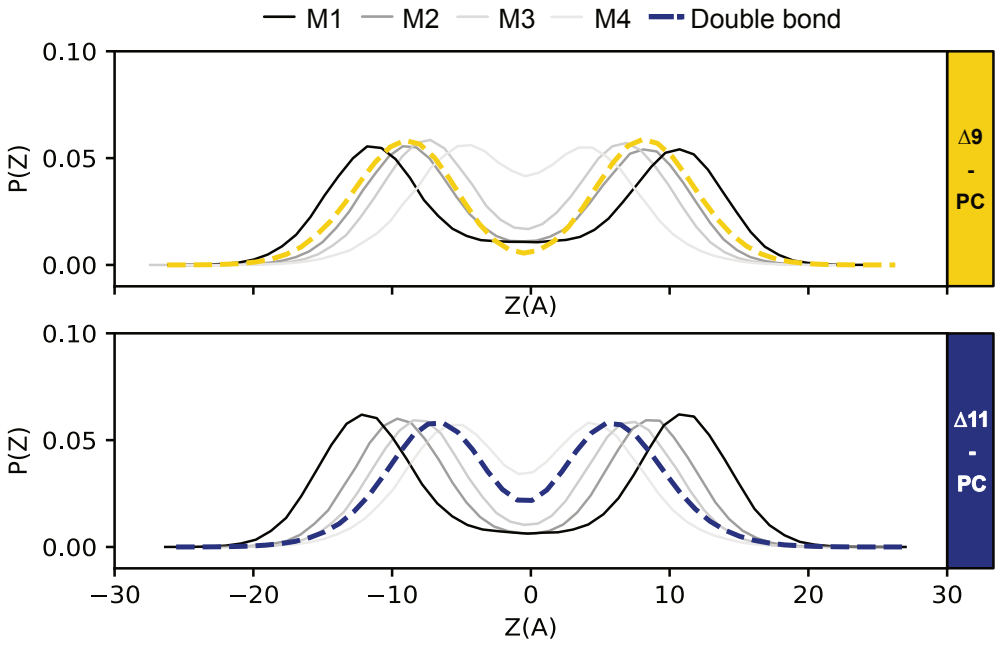

Fig 4. Overlapping distribution of Dpop's methyl groups and PC's double bond correspond to a reduced ordering effect. (A) The double bond in Δ9-PC overlaps with Dpop M2, preventing efficient lipid packing. (B) No Dpop methyl group overlap with the double bond of Δ11-PC.

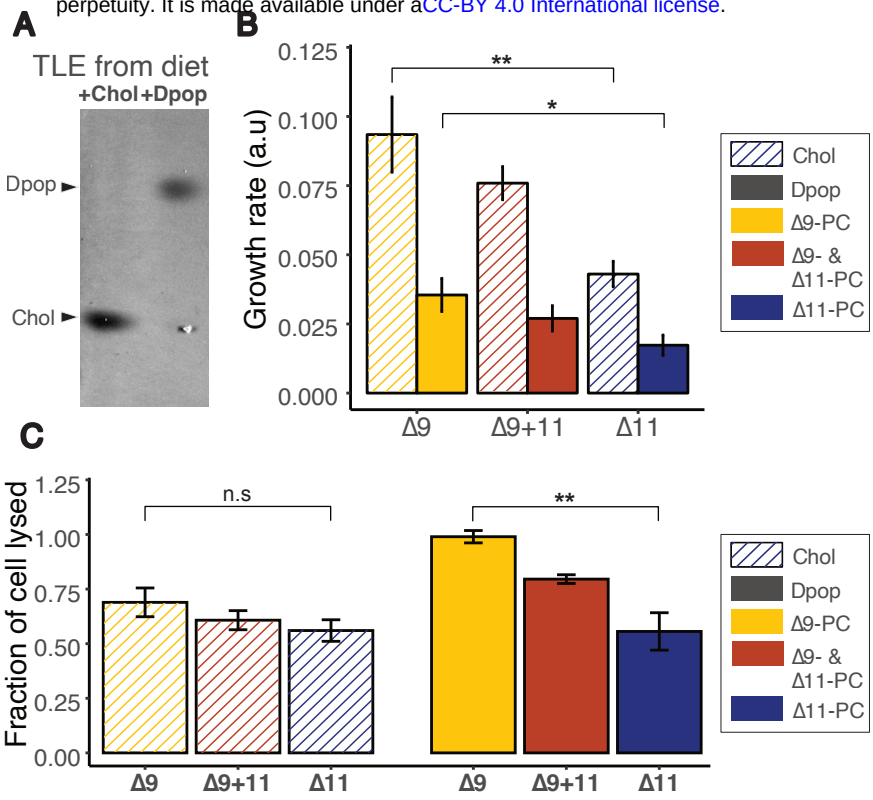

Fig 5. Dpop and Δ11-PC enhance robustness of Mesoplasma florum to hypoosmotic shock compared with Dpop and Δ9-PC. (A) Chol and Dpop were incorporated into Mesoplasma membranes according to their respective diets (B) Growth rate of M. florum on different diets. ** ($F=24.4$, $p < 0.005$) * ($F=10.6$, $p < 0.05$) Analysis were performed using one-sided anova with Tukey post hoc test (C) Membrane robustness reflected by the fraction of cell lysed when subjected to hypoosmotic shock. n.s ($F=1.47$, $p<0.5$) ** ($F=16.6$, $p < 0.005$) Analysis were performed using one-sided anova with Tukey post hoc test.